

# The first binary star evolution model producing a Chandrasekhar mass white dwarf

S.-C. Yoon and N. Langer

Astronomical Institute, Utrecht University, Princetonplein 5, 3584 CC, Utrecht, The Netherlands

Received 25 September 2003 / Accepted 6 November 2003

**Abstract.** Today, Type Ia supernovae are essential tools for cosmology, and recognized as major contributors to the chemical evolution of galaxies. The construction of detailed supernova progenitor models, however, was so far prevented by various physical and numerical difficulties in simulating binary systems with an accreting white dwarf component, e.g., unstable helium shell burning which may cause significant expansion and mass loss. Here, we present the first binary evolution calculation which models both stellar components and the binary interaction simultaneously, and where the white dwarf mass grows up to the Chandrasekhar limit by mass accretion. Our model starts with a  $1.6 M_{\odot}$  helium star and a  $1.0 M_{\odot}$  CO white dwarf in a 0.124 day orbit. Thermally unstable mass transfer starts when the CO core of the helium star reaches  $0.53 M_{\odot}$ , with mass transfer rates of  $1 \cdot \cdot \cdot 8 \times 10^{-6} M_{\odot}/\text{yr}$ . The white dwarf burns the accreted helium steadily until the white dwarf mass has reached  $\sim 1.3 M_{\odot}$  and weak thermal pulses follow until carbon ignites in the center when the white dwarf reaches  $1.37 M_{\odot}$ . Although the supernova production rate through this channel is not well known, and this channel can not be the only one as its progenitor life time is rather short ( $\sim 10^7$ – $10^8$  yr), our results indicate that helium star plus white dwarf systems form a reliable route for producing Type Ia supernovae.

**Key words.** stars: evolution – stars: white dwarf – stars: helium – stars: binary – stars: supernova – supernovae: Type Ia

## 1. Introduction

Type Ia supernovae (SNe Ia) are of particular importance in astrophysics: They are the major source for iron group elements in the universe and are thus an essential contributor to the chemical evolution of galaxies (e.g. Renzini 1999). And their light curve properties allow it to measure their distances with an excellent accuracy even out to redshifts beyond  $z = 1$ , which makes them a powerful tool to determine the cosmological parameters (e.g. Hamuy et al. 1996; Branch 1998; Leibundgut 2000). In particular, the recent suggestion of a non-zero cosmological constant is in part based on SNe Ia data (Perlmutter et al. 1999; Riess et al. 2000). An understanding of the progenitors of these supernovae is clearly required as a basis for these fundamental astrophysical phenomena.

However, even though there seems no doubt that SNe Ia are produced by the thermonuclear explosion of a white dwarf, it is currently unclear in which kinds of binary systems such an event can occur (Livio 2001). Among the scenarios which have been put forward as possibilities, the so called single degenerate scenario is currently favored, where a CO white dwarf accretes mass from a non-degenerate companion and thereby grows up to the Chandrasekhar mass (e.g. Hillebrandt & Niemeyer 2000; Livio 2001). However, hydrogen as well as helium accretion rates which allow an increase of the CO white

dwarf mass due to shell burning are limited to narrow ranges (e.g. Nomoto 1982; Fujimoto 1982; Iben & Tutukov 1989). While hydrogen and helium shell sources are prone to degeneracy effects and related thermonuclear instabilities (e.g., nova explosions) at low accretion rates, the helium shell source in accreting white dwarf models has been found to be thermally unstable even for cases where the electron degeneracy is negligible (e.g. Cassisi et al. 1998; Langer et al. 2002). This affects in particular the potentially most frequent SN Ia progenitor systems, where a hydrogen rich star (main sequence star or red giant) is considered as white dwarf companion (e.g. Li & van den Heuvel 1997; Hachisu et al. 1999; Langer et al. 2000). The hydrogen accretion rates in those systems which may allow steady hydrogen shell burning are about a few  $10^{-7} M_{\odot}/\text{yr}$ . With these rates, the subsequent helium shell burning is usually found to be unstable (Iben & Tutukov 1989; Cassisi et al. 1998; Kato & Hachisu 1999), and no model sequences which cover the major part of the white dwarf accretion phase could be constructed so far.

In an effort towards overcoming this shortcoming, we consider here the evolution of close helium star plus CO white dwarf systems. In those, the white dwarf develops only a helium shell source, thus avoiding complications involved in double shell source models (e.g. Iben & Tutukov 1989). Such systems form a predicted binary evolution channel (Iben & Tutukov 1994), which is confirmed – even though for lower masses than considered here – by Maxted et al. (2000). Further

Send offprint requests to: S.-C. Yoon,  
e-mail: S.C.Yoon@astro.uu.nl

evidence for the existence of close helium star plus CO white dwarf systems comes from the recent discovery of a helium nova (Ashok & Banerjee 2003; Kato & Hachisu 2003).

Simplified binary evolution considerations provided us with an estimate for the optimal initial parameters of our model system. As a result, we embarked on calculating the detailed evolution of a  $1.6 M_{\odot}$  helium star and a  $1 M_{\odot}$  CO white dwarf in a 0.124 d orbit. We introduce our computational method and physical assumptions in Sect. 2. In Sect. 3, the evolution of the considered binary system is presented. We discuss our results in Sect. 4.

## 2. Numerical method and physical assumptions

The numerical model has been computed with a binary stellar evolution code which computes the evolution of two binary components, and the evolution of the mass transfer rate and of the orbital separation simultaneously through an implicit coupling scheme (Braun 1997). We use Eggleton's (1983) approximation for the Roche lobe radius. Mass loss from the Roche lobe filling star through the first Lagrangian point is computed according to Ritter (1988). The orbital change due to stellar wind and mass transfer is followed according to Podsiadlowski et al. (1992). The specific angular momentum carried away by the stellar wind is computed following Brookshaw & Tavani (1993). Orbital angular momentum loss due to the gravitational wave radiation is also taken into account. Opacities are taken from Iglesias & Rogers (1996). Mass loss due to a stellar wind is considered as  $\dot{M} = 10^{-2} RL/[GM(1 - \Gamma)]$ , with  $\Gamma$  being the ratio of photospheric to Eddington luminosity. This mass loss rate is based on dimensional arguments and normalized for Wolf-Rayet stars (Langer 1989). However, the particular choice of the stellar wind mass loss formula does not affect our final results significantly, given that the value of the mass loss rate is largely determined by  $\Gamma$ , as the luminosity of the white dwarf during the mass accretion phase is close to the Eddington limit. Effects of rotation are not considered here (cf. Langer et al. 2002; Yoon et al. 2004). For more details about the code, see Wellstein & Langer (1999) and Wellstein et al (2001).

We start with a zero age main sequence helium star of  $1.6 M_{\odot}$  and a  $1.0 M_{\odot}$  white dwarf, in 0.124 day orbit. The metallicity of the helium star is set to 0.02. In order to avoid the numerical difficulty in following the initial strong helium shell flash in the white dwarf which might be induced soon after the onset of mass accretion, the white dwarf is approximated by a point mass until the mass transfer rate from the helium star reaches about  $10^{-6} M_{\odot}/\text{yr}$  (see Fig. 3 in Sect. 3). To mimic the heating by the initial shell flash, we exchange the point mass by a hot and bright ( $\log L_s/L_{\odot} = 4.175$ ) white dwarf model at this time. The initial central temperature and density of the white dwarf are  $T_c = 1.8 \times 10^8$  K and  $2 \times 10^7$  g/cm<sup>3</sup> respectively. Although the central temperature may be much lower in reality when the mass accretion starts, the initial temperature structure is unimportant for the advanced evolution due to the self-heating of the white dwarfs (cf. Sect. 3).

The calculations presented here required high space and time resolution: About 500 000 binary models were computed, where both stars were resolved into  $\sim 1000$  mass shells.

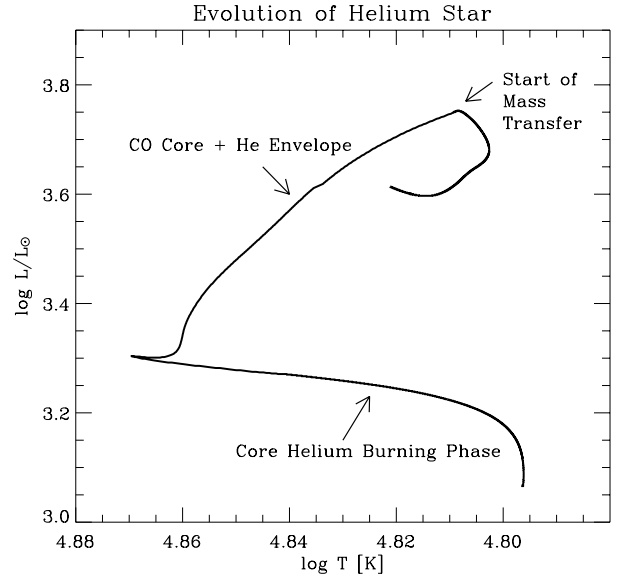


Fig. 1. Evolution of the  $1.6 M_{\odot}$  helium star in the HR diagram.

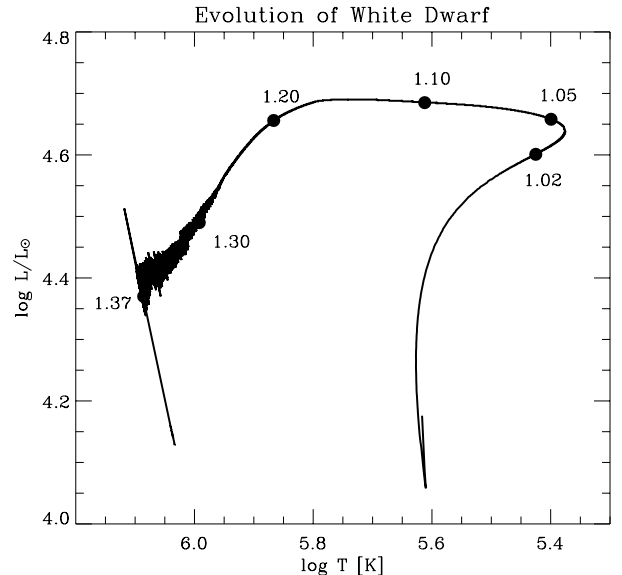


Fig. 2. Evolution of the CO white dwarf during the mass accretion phase in the HR diagram. The numbers at the filled circles denote the white dwarf mass in the unit of solar mass at the given points.

## 3. Results

The evolution of our  $1.6 M_{\odot}$  helium star +  $1 M_{\odot}$  CO white dwarf binary system proceeds as follows (see Figs. 1 and 2, and Table 1). The helium star undergoes the core helium burning for 4.28 million years. After core helium exhaustion, the envelope of the helium star expands and starts to fill its Roche lobe (Fig. 1) when the radius of the helium star reaches  $0.61 R_{\odot}$ . At this point, the CO core mass of the helium star reaches  $0.53 M_{\odot}$  and mass transfer from the helium star commences. Even though at this time the helium star expands on the nuclear timescale of helium shell burning, the mass transfer shrinks the orbit and thus proceeds on the thermal timescale of the helium star. The resulting mass transfer rates are in the range  $1 \dots 8 \times 10^6 M_{\odot}/\text{yr}$ , as shown by the dotted line in Fig. 3.

**Table 1.** Component masses, orbital period, and central density of both stars, for five different times during the mass transfer, including the beginning of mass transfer (defines  $t = 0$ ), the time of minimum orbital separation ( $t = 73\,000$  yr), and the time of central carbon ignition ( $t = 148\,000$  yr).

$t$	$M_{\text{He}}$	$M_{\text{WD}}$	$P$	$\rho_{\text{c,He}}$	$\rho_{\text{c,WD}}$
$10^3$ yr	$M_{\odot}$	$M_{\odot}$	h	$10^5 \text{ g cm}^{-3}$	$10^8 \text{ g cm}^{-3}$
0	1.60	1.00	2.97	1.31	0.20
35	1.39	1.10	2.70	1.53	0.51
73	1.25	1.21	2.65	1.86	1.45
110	1.15	1.30	2.69	2.30	4.70
148	1.08	1.37	2.78	2.92	23.5

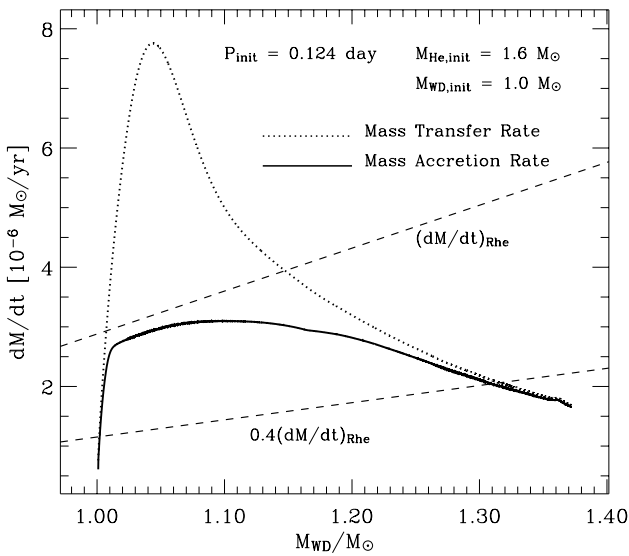


**Fig. 3.** Mass transfer rate (dotted line) and white dwarf mass accretion rate (solid line) as function of the white dwarf mass, for the considered binary model. The upper dashed line denotes the critical mass accretion rate above which the helium envelope is expected to expand to giant dimensions (Nomoto 1982). For accretion rates below the lower dashed line helium shell burning is usually unstable.

A part of the transferred matter is blown off by the stellar wind at the white dwarf surface without being burned into carbon and oxygen, and thus without affecting the thermal evolution of the CO core. The rest is transformed into CO in the helium burning shell source and accreted into the CO core. As the mass transfer rate from the helium star increases, the surface luminosity of the white dwarf reaches about 40% of its Eddington luminosity (see Fig. 2). A radiation driven wind from the white dwarf surface is induced, with a peak of  $4.8 \times 10^{-6} M_{\odot}/\text{yr}$  at  $M_{\text{WD}} \approx 1.04 M_{\odot}$ . As the mass transfer rate decreases, the stellar wind from the white dwarf becomes weaker. The upper dashed lines in Fig. 3 denotes the critical mass accretion rate above which the helium envelope is expected to expand to giant dimensions,  $\dot{M}_{\text{Rhe}} = 7.2 \times 10^{-6} (M_{\text{CO}}/M_{\odot} - 0.60) M_{\odot}/\text{yr}$ , based on white dwarf models computed with constant mass accretion rates (Nomoto 1982). The helium shell source is expected to be stable when  $0.4\dot{M}_{\text{Rhe}} < \dot{M} < \dot{M}_{\text{Rhe}}$ . The accretion rate in the white dwarf remains in the steady helium shell burning regime until  $M \approx 1.3 M_{\odot}$  and the white dwarf mass grows efficiently

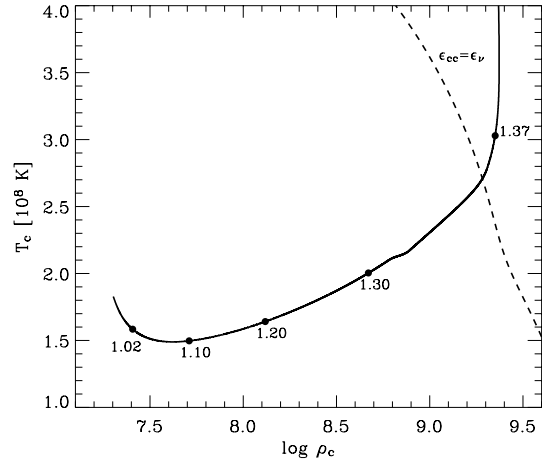


**Fig. 4.** Evolution of central density and temperature in the white dwarf during the mass accretion phase. The dashed line gives the locus where the energy generation rate due to the carbon burning equals to the neutrino cooling rate. The numbers at the filled circles denote the white dwarf mass in the unit of solar mass at the given points.

(Fig. 2). Thereafter, the white dwarf undergoes weak thermal pulses.

During the mass accretion, the surface temperature of the white dwarf varies from  $2.5 \times 10^5$  K to  $12 \times 10^5$  K and the luminosity reaches  $2.5 \dots 5 \times 10^4 L_{\odot}$  (Fig. 2), with which the white dwarf will appear as a super-soft X-ray source (e.g. Kahabka & van den Heuvel 1997; Greiner 2000). The central temperature of the white dwarf decreases initially, mainly due to neutrino emission. When  $M_{\text{WD}} \gtrsim 1.1 M_{\odot}$ , the compressional heating begins to dominate, and the central temperature of the white dwarf increases. The dashed line in Fig. 4 indicates where the energy generation rate due to the carbon burning equals to the neutrino energy loss rate. The white dwarf reaches this line at  $\rho_{\text{c}} = 1.92 \times 10^9 \text{ g/cm}^3$  and  $T_{\text{c}} = 2.71 \times 10^8$  K, from where the central temperature increases rapidly. About 1700 years thereafter, when  $T_{\text{c}} \approx 2.9 \times 10^8$  K, the central region becomes convectively unstable. About 1800 years later, in our last model, the convection zone extends to  $\approx 0.5 M_{\odot}$  when  $T_{\text{c}} = 4.6 \times 10^8$  K (Fig. 5).

The convective URCA process, which is not considered in our study, may affect the evolution during this stage (Paczynski 1972; Iben 1982). It is currently still debated whether it leads to heating or to cooling of the convective core (e.g. Mochkovitch 1996; Stein et al. 1999). Thus we have to consider the spatial extent and duration of the convective phase, as obtained from our models, as uncertain. When the temperature exceeds  $5 \dots 8 \times 10^8$  K, the nuclear time scale becomes comparable to the convective time scale. In this case, convection is not able to efficiently carry away the released nuclear energy, and the mixing length theory becomes inadequate to describe the convective energy transport. Therefore, we stop the calculation at this point; see, however, Höflich & Stein (2002) for the further evolution.

In our last model, the helium star has a mass of  $1.08 M_{\odot}$  and a CO core mass of  $0.64 M_{\odot}$ . If the white dwarf explodes, the helium star may survive but suffer stripping off small amounts of mass by the supernova ejecta (Marrietta et al. 2000). Its space

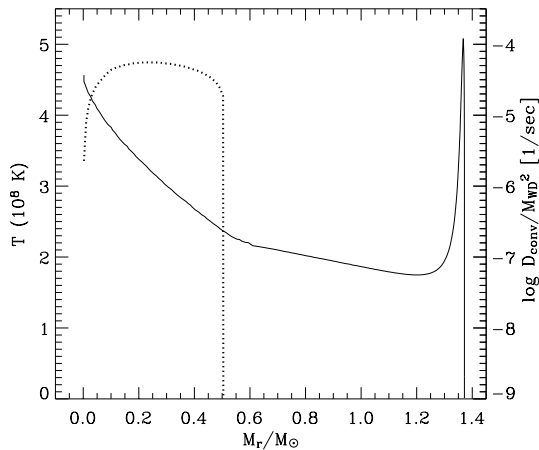


**Fig. 5.** Temperature as function of the mass coordinate in the last white dwarf model. The dotted lines show the convective diffusion coefficient (in the unit of  $\text{g}^2/\text{s}$ ) divided by the square of the total mass of the white dwarf.

velocity will be close to its final orbital velocity of  $330 \text{ km s}^{-1}$ . It will evolve into a massive CO white dwarf of  $\sim 1.0 M_{\odot}$  eventually.

#### 4. Discussion

The model described above is (to our knowledge) the first self-consistent binary evolution calculation which leads to a Chandrasekhar-mass white dwarf. Its relevance is in part the realistic construction of a supernova progenitor white dwarf model, but even more the fact that it provides for the first time hard evidence of the functioning of a SN Ia progenitor channel: Our results leave little doubts that some helium star plus white dwarf systems will in fact produce a Type Ia supernova.

The considered system may have evolved from a wide  $8.0 M_{\odot}$  giant star +  $1.0 M_{\odot}$  white dwarf system though a common envelope phase, which in turn may be the result of two intermediate mass stars in a close orbit. This indicates a system life time of the order of  $\sim 10^7$ – $10^8$  yr, which is too short to explain SNe Ia in elliptical galaxies. Therefore, our results support the idea that at least two SN Ia progenitor scenarios are realized in nature (e.g., della Valle & Livio 1994). Iben & Tutukov (1994) estimated the potential SN Ia production rate through white dwarf + helium giant binary systems to  $1.7 \times 10^{-3} \text{ yr}^{-1}$ , which may constitute a significant fraction of SNe Ia observed in late type galaxies.

As previously mentioned, SNe Ia progenitors of the kind considered here will appear as a super-soft X-ray source (SSS). We note that, since a wide range of orbital separations is possible for helium star plus white dwarf systems (Iben & Tutukov 1994), this may explain SSSs with various orbital periods. For instance, short period systems such as RX J0537.7-7034 (3.5h, Greiner et al. 2000) and 1E0035.4-7230 (4.1h, Schmidtke et al. 1996) can not be easily explained within the canonical model which invokes hydrogen rich donor stars (e.g., Rappaport et al. 1994; Kahabka and van den Heuvel 1997), except at low metallicity (Langer et al. 2000). Orbital periods of the binary system in the present study in the range 2.65–2.97 h indicate

that helium star plus white dwarf systems might be another natural possibility to explain short period SSSs.

*Acknowledgements.* We thank the referee for pointing out to us the recent discovery of a helium nova. SCY is grateful to Philipp Podsiadlowski for many helpful discussions during his visit to Oxford in February 2003, where this work was initiated. This research has been supported in part by the Netherlands Organization for Scientific Research (NWO).

#### References

- Ashok, N. M., & Banerjee, D. P. K. 2003, *A&A*, 409, 1007  
 Branch, D. 1998, *ARA&A*, 36, 17  
 Braun, H. 1997, Ph.D. Thesis, LMU München  
 Brookshaw, L., & Tavani, M. 1993, *ApJ*, 410, 719  
 Cassisi, S., Iben, I., & Tornambé, A. 1998, *ApJ*, 469, 376  
 della Valle, M., & Livio, M. 1994, *ApJ*, 423, L31  
 Eggleton, P. 1983, *ApJ*, 268, 368  
 Fujimoto, M. Y. 1982, *ApJ*, 257, 767  
 Greiner, J. 2000, *New Astron.*, 5, 137  
 Greiner, J., Orio, M., & Schwarz, R. 2000, *A&A*, 355, 1041  
 Hachisu, I., Kato, M., & Nomoto, K. 1999, *ApJ*, 522, 487  
 Hamuy, M., Phillips, M. M., Suntzeff, N. B., et al. 1996, *ApJ*, 519, 314  
 Hillebrandt, W., & Niemeyer, J. C. 2000, *ARA&A*, 38, 191  
 Höflich, P., & Stein, J. 2002, *ApJ*, 568, 779  
 Iben, I. Jr. 1982, *ApJ*, 253, 248  
 Iben, I. Jr., & Tutukov, A. V. 1989, *ApJ*, 342, 430  
 Iben, I. Jr., & Tutukov, A. V. 1994, *ApJ*, 431, 264  
 Iglesias, C. A., & Rogers, F. J. 1996, *ApJ*, 464, 943  
 Kahabka, P., & van den Heuvel, E. P. J. 1997, *ARA&A*, 35, 69  
 Kato, M., & Hachisu, I. 1999, *ApJ*, 513, L41  
 Kato, M., & Hachisu, I. 2003, to appear in *ApJL* [astro-ph/0310351]  
 Langer, N. 1989, *A&A*, 210, 93  
 Langer, N., Deutschmann, A., Wellstein, S., & Höflich, P. 2000, *A&A*, 362, 1046  
 Langer, N., Yoon, S.-C., Wellstein, S., & Scheithauer, S. 2002, *ASP Conf. Proc.* 261, ed. B. T. Gaensicke et al., 252  
 Leibundgut, B. 2000, *A&AR*, 10, 179  
 Li, X.-D., & van den Heuvel, E. P. J. 1997, *A&A*, 322, L9  
 Livio 2001, in *Cosmic evolution*, ed. E. Vangioni, R. Ferlet, M. Lemoine (New Jersey: World Scientific)  
 Marrietta, E., Burrows, A., & Fryxell, B. 2000, *ApJS*, 218, 615  
 Maxted, P. F. L., March, T. R., & North, R. C. 2000, *MNRAS*, 317, L41  
 Mochkovitch, R. 1996, *A&A*, 311, 152  
 Nomoto, K. 1982, *ApJ*, 253, 798  
 Paczyński, B. 1972, *ApJ*, L11, 53  
 Perlmutter, S., Aldering, G., Goldhaber, G., et al. 1999, *ApJ*, 517, 565  
 Podsiadlowski, Ph., Joss, P. C., & Hsu, J. J. L. 1992, *ApJ*, 391, 246  
 Rappaport, S. A., Di Stefano, R., & Smith, M. 1994, *ApJ*, 426, 692  
 Renzini, A. 1999, in *Chemical Evolution from Zero to High Redshift* (Heidelberg: Springer Verlag), 185  
 Riess, A. G., Filippenko, A. V., Liu, M. C., et al. 2000, *ApJ*, 536, 62  
 Ritter, H. 1988, *A&A*, 202, 93  
 Schmidtke, P. C., Cowley, A. P., McGrath, T. K., Hutchings, J. B., & Crampston, D. 1996, *AJ*, 111, 788  
 Stein, J., Barkat, Z., & Wheeler, J. C. 1999, *ApJ*, 523, 381  
 Wellstein, S., & Langer, N. 1999, *A&A*, 350, 148  
 Wellstein, S., Langer, N., & Braun, H. 2001, *A&A*, 369, 939  
 Yoon, S.-C., Langer, N., & Scheithauer, S. 2004, *A&A*, in preparation